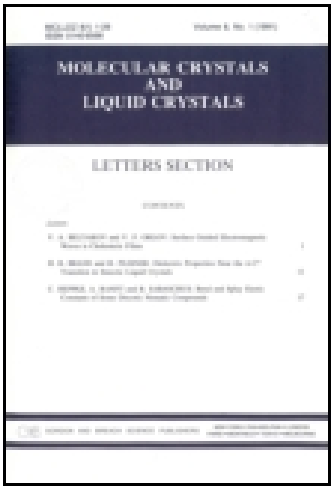

Molecular Crystals and Liquid Crystals
Publication details, including instructions for authors and subscription information:
http://www.tandfonline.com/loi/gmcl20

Mechanochromic Photoluminescent Liquid Crystals Containing 5,5′-Bis(2-phenylethynyl)-2,2′-bithiophene

Masato Mitani[a], Shogo Yamane[a], Masafumi Yoshio[a], Masahiro Funahashi[ab] & Takashi Kato[a]

[a] Department of Chemistry and Biotechnology, School of Engineering, The University of Tokyo, Hongo, Bunkyo-ku, Tokyo, Japan

[b] Department of Advanced Materials Science, Faculty of Engineering, Kagawa University, Hayashi-cho, Takamatsu, Kagawa, Japan

Published online: 30 Sep 2014.

To cite this article: Masato Mitani, Shogo Yamane, Masafumi Yoshio, Masahiro Funahashi & Takashi Kato (2014) Mechanochromic Photoluminescent Liquid Crystals Containing 5,5′-Bis(2-phenylethynyl)-2,2′-bithiophene, Molecular Crystals and Liquid Crystals, 594:1, 112-121, DOI: 10.1080/15421406.2014.917499

To link to this article: http://dx.doi.org/10.1080/15421406.2014.917499

Mol. Cryst. and Liq. Cryst., Vol. 594: pp. 112–121, 2014

ISSN: 1542-1406 print/1563-5287 online
DOI: 10.1080/15421406.2014.917499

Taylor & Francis
Taylor & Francis Group

Mechanochromic Photoluminescent Liquid Crystals Containing 5,5′-Bis(2-phenylethynyl)-2,2′-bithiophene

MASATO MITANI,[1] SHOGO YAMANE,[1]
MASAFUMI YOSHIO,[1] MASAHIRO FUNAHASHI,[1,2]
AND TAKASHI KATO[1,*]

[1]Department of Chemistry and Biotechnology, School of Engineering, The University of Tokyo, Hongo, Bunkyo-ku, Tokyo, Japan
[2]Department of Advanced Materials Science, Faculty of Engineering, Kagawa University, Hayashi-cho, Takamatsu, Kagawa, Japan

*5,5′-Bis(2-phenylethynyl)-2,2′-bithiophene derivative **1** containing dendritic moieties linked through amide groups was synthesized. Compound **1** exhibits a rectangular columnar phase on slow cooling from the isotropic liquid. In contrast, a cubic phase is formed as a metastable liquid-crystalline phase by rapid cooling of the isotropic melt. Mechanical shearing induces a cubic–columnar phase transition, accompanied by the change of a photoluminescent color from yellow-green to green. The infrared spectra of **1** suggest that the mechanical stimuli can induce the partial dissociation of the hydrogen bond. This may lead to more disordering of the π-stacks of chromophores.*

Keywords Mechanochromic photoluminescence; stimuli-responsive material; bithiophene

Introduction

Mechanochromic photoluminescent materials change their luminescent properties on the basis of the change of their assembled structures induced by the mechanical stimuli. These materials have attracted much attention because they have potential applications as displays, memories, and sensors [1–11]. However, it is difficult to establish general design of mechanochromic molecules. Liquid-crystalline (LC) materials [12–22] are self-assembled anisotropic fluids which can be easily and dynamically controlled by applying the external stimuli [3, 7, 23–27]. Recently nanostructured [17–27] liquid crystals exhibiting cubic, smetic, and columnar phases have been studied intensively as functional materials. We reported on the stimuli-responsive photoluminescent nanostructured liquid crystals based on photoluminescent pyrene [3, 7], anthracene [23, 24] and naphtharene [25] moieties. These materials change their photoluminescent colors on the changes of the assembled structures of the π-conjugated moieties accompanied with the cubic–columnar LC phase transitions. On the other hand, the assembled structures of π-conjugated moieties greatly

*Address correspondence to Takashi Kato, Department of Chemistry and Biotechnology, School of Engineering, The University of Tokyo, Hongo, Bunkyo-ku, Tokyo 113-8656, Japan. Phone: +81-3-5841-7440. Fax: +81-3-5841-8661; E-mail: kato@chiral.t.u-tokyo.ac.jp

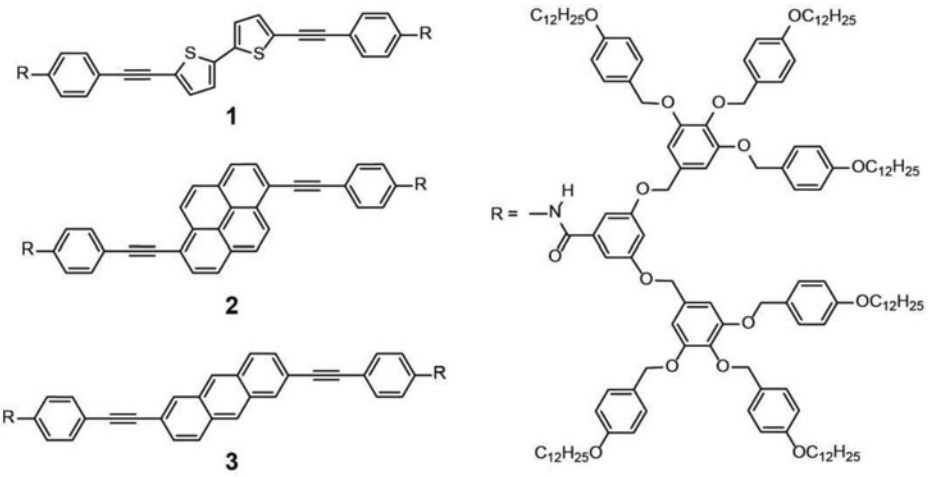

Figure 1. Molecular structures of compounds **1**, **2** (Refs. [3]), and **3** (Refs. [23]).

affect the carrier mobility of the organic semiconductors [28–34]. By using our strategy, not only its photoluminescent color but also its carrier mobility of the material can be controlled by the mechanical stimuli. Herein we report on a mechanochromic photoluminescent liquid crystal based on a bithiophene moiety. Oligothiophene derivatives have been intensively studied because of their hole transport abilities in addition to their photoluminescent properties [35–38]. Although we previously reported columnar [31, 34] and smectic [32] LC oligothiophene derivatives showing efficient 1D and 2D hole transport properties, respectively, no LC oligothiophene derivative showing stimuli-responsive behavior was reported.

We have designed compound **1** containing a 5,5′-bis(2-phenylethynyl)-2,2′-bithiophene moiety as the photoluminescent core (Fig. 1). As an electronic material, 5,5′-bis(2-phenylethynyl)-2,2′-bithiophene was reported to exhibit the hole mobility of 2.8×10^{-2} cm^2 V^{-1} s^{-1} in the organic field effect transistor device by Hu and coworkers [39]. Mechanochromic photoluminescent liquid crystals **2** and **3**, which were previously reported are depicted in Fig. 1.

Experimental

General Methods and Materials

All reagents and solvents were purchased from Aldrich, Junsei Kagaku, Tokyo Kasei, and Wako. All of the reactions were carried out under argon atmosphere in dry solvents. Silica gel column chromatography was carried out with silica gel 60 from Kanto Chemicals (silica gel 60, spherical, 40–50 μm). Recycling preparative GPC was carried out with a Japan Analytical Industry LC-9201 chromatograph. ^{1}H and ^{13}C NMR spectra were obtained using a JEOL JNM-LA400 at 400 and 100 MHz in $CDCl_3$, respectively. Chemical shifts of ^{1}H and ^{13}C NMR signals were quoted to internal standard Me_4Si and expressed by chemical shifts in ppm (δ), multiplicity, coupling constant (Hz), and relative intensity. Elemental analyses were carried out with an Exeter Analytical Inc. CE-440 Elemental Analyzer. Differential

scanning calorimetry (DSC) measurements (scanning rate of 10 K min^{-1}) were conducted with a NETZSCH DSC204 Phoenix differential scanning calorimeter. An Olympus BH-2 polarizing optical microscope (POM) equipped with a Mettler FP82HT hot-stage was used to verify thermal transitions and characterize anisotropic textures. X-ray diffraction measurements were carried out on Rigaku RINT 2500 diffractometer with a heating stage using Ni-filtered Cu Kα radiation and Rigaku SmartLab. IR measurements were conducted on a JASCO FT/ IR-660 Plus using CaF_2 plates. UV-vis absorption spectra were obtained with a Jasco V-670 equipped with an integrating sphere unit ISN-800T. Steady-state fluorescence spectra were recorded on a Jasco FP-6500 spectrofluorometer equipped with a hot stage.

Synthesis

5,5′-Diethynyl-2,2′-bithiophene and *N*-4-iodophenyl 3,5-bis{3′,4′,5′-tris[*p*-(dodecan-1-yloxy)benzyloxy]benzyloxy}benzamide were obtained according to the reported procedures [3, 40].

*5,5′-Bis[p-(3,5-bis{3′,4′,5′-tris[p-(dodecan-1-yloxy)benzyloxy]benzyloxy}benzamide) phenylethynyl]-2,2′-bithiophene (**1**).* To a suspension of *N*-4-iodophenyl 3,5-bis{3′,4′,5′-tris[*p*-(dodecan-1-yloxy)benzyloxy]benzyloxy}benzamide (260 mg, 0.114 mmol), 5,5′-diethynyl-2,2′-bithiophene (11.1 mg, 5.18×10^{-2} mmol), dry toluene (7 ml), and freshly distilled Et_3N (3.5 ml) was added CuI (1.0 mg, 5.2×10^{-3} mmol) and $Pd(PPh_3)_4$ (6.0 mg, 5.2×10^{-3} mmol). The mixture was stirred for 16 h at 60°C, and then the reaction mixture was poured into a mixture of 5% hydrochloric acid and chloroform. The organic layer was separated, washed with saturated $NaHCO_3$ aqueous solution, H_2O, and saturated NaCl aqueous solution, then dried over $MgSO_4$. After filtration and evaporation, the product was purified by silica gel chromatography (eluent: chloroform/hexane = 3:1) and GPC (eluent: chloroform) to afford **1** as a transparent yellow solid (yield = 60 mg, 26%). ^{1}H NMR (400 MHz, $CDCl_3$): δ 7.84 (s, 2H), 7.66 (d, J = 8.8 Hz, 4H), 7.51 (d, J = 8.8 Hz, 4H), 7.32–7.27 (m, 24H), 7.17 (d, J = 3.2 Hz, 2H), 7.09 (d, J = 4.0 Hz, 2H), 7.02 (d, J = 2.0 Hz, 4H), 6.86 (d, J = 8.8 Hz, 16H), 6.76 (d, J = 7.2 Hz, 8H), 6.73 (m, 2H), 6.71 (s, 8H), 5.02 (s, 16H), 4.98 (s, 8H), 4.94 (s, 8H), 3.97–3.90 (m, 24H), 1.81–1.74 (m, 24H), 1.46–1.41 (m, 24H), 1.26 (m, 192H), 0.89–0.86 (m, 36H). ^{13}C{^{1}H} NMR (100 MHz, $CDCl_3$): δ 165.32, 160.05, 158.92, 153.17, 138.45, 138.18, 138.00, 137.00, 132.71, 132.32, 131.57, 130.21, 129.82, 129.13, 128.85, 123.96, 122.66, 119.63, 118.59, 114.42, 114.10, 107.36, 106.21, 105.44, 94.33, 82.40, 74.82, 71.17, 70.51, 68.07, 67.98, 31.91, 29.67, 29.63, 29.62, 29.60, 29.54, 29.45, 29.35, 29.31, 26.08, 22.68, 14.10. Elemental analysis: Calcd. (%) for $C_{294}H_{408}N_2O_{30}S_2$: C, 78.22; H, 9.11; N, 0.62. Found: C, 78.31; H, 8.94; N, 0.78.

Results and Discussion

Compound **1** has dendritic moieties [41] attached to the photoluminescent core. This molecular design is similar to those of previously reported compounds **2** and **3** that show both the cubic (Cub) phase and the columnar (Col) phase [3, 23–25]. It was expected that compound **1** showed the cubic phase and columnar phase. Compound **1** shows different LC phases depending on the cooling process from the isotropic phase. Compound **1** shows a blue-green emission in the isotropic (Iso) phase (Fig. 2(a)). A slow cooling process of compound **1** from the isotropic phase leads to the formation of the rectangular columnar (Col_r) phase (Fig. 2(b)). Compound **1** shows green photoluminescence in the rectangular

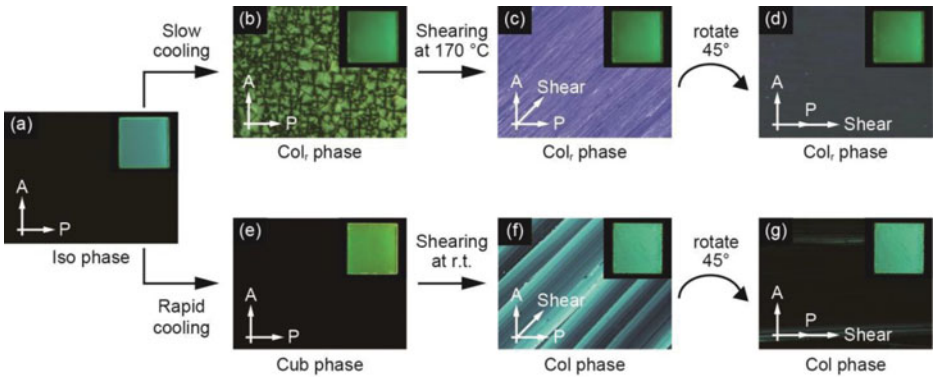

Figure 2. Polarizing microscopic images of compound **1** and its photoluminescent color (inset): (a) in the isotropic phase at 200°C; (b) in the rectangular columnar phase at 170°C; (c,d) in the rectangular columnar phase at 170°C after shearing; (e) in the cubic phase at r.t. and (f,g) in the shear-induced columnar phase at r.t. Photoluminescent images of compound **1** were obtained for the samples sandwiched between quartz substrates under UV irradiation at 365 nm in each condition. Arrows indicate the direction of the mechanical shearing and polarizer (P) and analyzer (A) axes.

columnar phase. Compound **1** in the rectangular columnar phase can be aligned to some extent after compound **1** is mechanically sheared within the sandwiched quartz substrates (Fig. 2(c)). The birefringence of the aligned film alternately changes from light to dark upon 45° rotation under crossed Nicols condition (Fig. 2(d)). On the other hand, the cubic phase is obtained by rapid cooling process from the isotropic phase to room temperature, and yellow-green photoluminescence is observed in the cubic phase (Fig. 2(e)). This LC behavior that is dependent on the cooling process from the isotropic phase was observed in the previously reported anthracene derivative **3** [23]. Mechanochromic luminescent properties of the compound **1** were examined. The photoluminescent color changes from yellow-green to green and compound **1** becomes to show the birefringence on POM observation after mechanical shearing is applied to compound **1** in the cubic phase (Fig. 2(f)). The shear-induced mesophase is so viscous that the uniformly aligned film cannot be obtained as indicated by the POM observations (Figs. 2(f),(g)). XRD measurements were carried out to identify the LC phases formed by compound **1**. For the rectangular columnar phase, two peaks in the small angle region are observed at 43.2 Å and 31.9 Å (Fig. 3(a)). These peaks correspond to the (20) and (22) reflection of a *P*2/*a* rectangular columnar phase (Col_r). This assumption is supported by the fact that previously reported pyrene derivative **2**, which has the same dendritic moieties, exhibits a *P*2/*a* rectangular columnar phase (Fig. 3(b)). For the cubic phase, two peaks in the small angle region at 47.4 Å and 33.1 Å are obtained (Fig. 3(c)). This feature is similar to the anthracene derivative **3** [23] (Fig. 3(d)). The peak at 47.4 Å can correspond to the (200), (210), and (211) reflections of a *Pm*3*n* micellar cubic phase. The XRD pattern shows one peak at 37.4 Å after shearing (Fig. 3(e)). The mesophase induced by the mechanical stimulus can be identified as the columnar phase because this behavior is also the same as that of the compound **3** (Fig. 3(f)) reported by us [23].

DSC measurements were carried out to examine the thermodynamic stabilities of LC phases formed by compound **1** (Fig. 4). Compound **1** exhibits the wide temperature range (54–179°C) of rectangular columnar phase (Table 1). An endothermic peak that corresponds to rectangular columnar–isotropic phase transition is observed at 179°C (Fig. 4(a)). On the

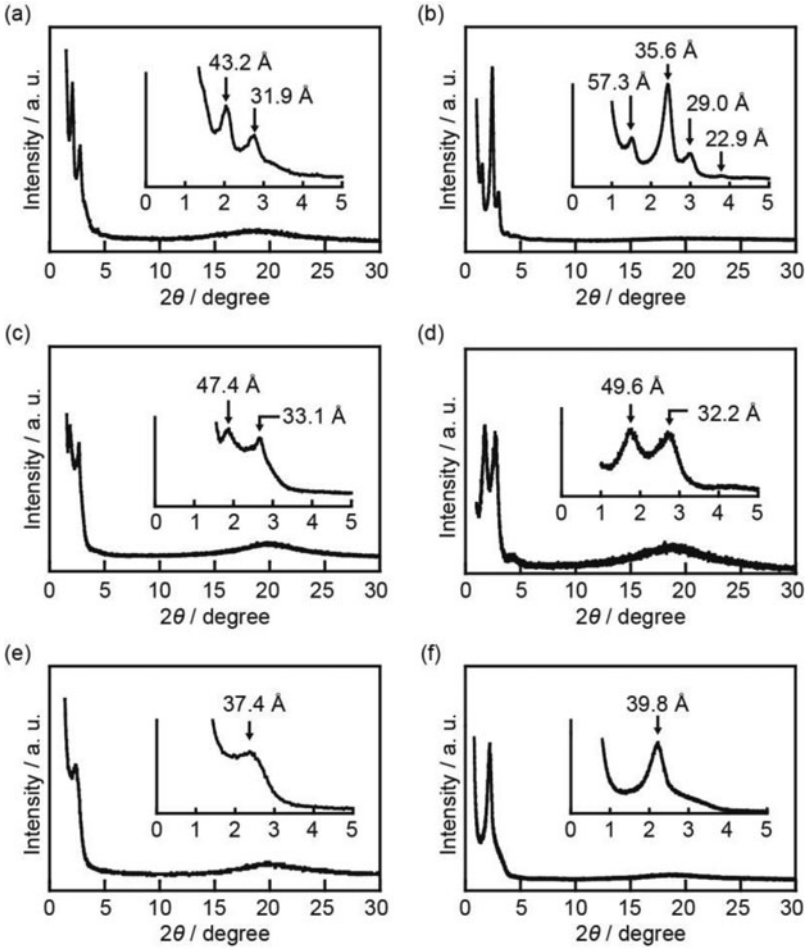

Figure 3. X-ray diffraction patterns: (a) compound **1** in the rectangular columnar phase at 170°C; (b) compound **2** in the rectangular columnar phase at 160°C; (c) compound **1** in the cubic phase at r.t.; (d) compound **3** in the cubic phase at 120°C; (e) compound **1** in the shear-induced columnar phase at r.t.; (f) compound **3** in the columnar phase at 120°C.

other hand, exothermic peaks corresponding to the phase transition to other mesophases (M) are observed in the cubic phase and the shear-induced columnar phase (Figs. 4(b),(c)). These exothermic peaks indicate that both the cubic phase and the shear-induced columnar phase are metastable.

Absorption and emission spectra of compound **1** were obtained to study the photoluminescent properties (Fig. 5). In the chloroform solution (1×10^{-5} M), compound **1** shows the absorption peak at 397 nm and the vibronic peaks in the emission spectra at 454 nm and 482 nm. In the isotropic phase, the absorption peak is observed at 390 nm and the emission peak is observed at 488 nm. Although the vibronic structure is not observed in the emission spectrum in the isotropic phase, the wavelength regions of the absorption and emission bands are almost the same as those in the solution state. On the other hand, the emission peak of compound **1** in the cubic phase shows the red-shift by 65 nm even though the absorption peak shows a little change on the isotropic–cubic phase transition. This large

Table 1. Thermal properties of compound **1**.

Sample	Phase transition behavior[a]
Sample after slow cooling from the isotropic phase	M 54 (52) Col_r 179 (133) Iso
Sample after rapid cooling from the isotropic phase	Cub 116 (–11) M 141 (–42) M 177 (134) Iso
Sheared sample in cubic phase at r.t.	Col 76 (–17) M 144 (–15) M 181 (144) Iso

[a]Transition temperatures (°C) were taken at the maximum in transition peaks detected by the differential scanning calorimetry (DSC) measurements on the first heating at the rate of 10°C min^{-1}. The transition enthalpies (kJ mol^{-1}) are in parentheses. M: unidentified mesophase; Col_r: rectangular columnar; Col: unidentified columnar; Cub: micellar cubic; Iso: isotropic.

red-shift can be caused by the formation of excimer in the cubic phase, which is observed in the previous molecules [3, 23–25]. The shoulder observed in the absorption spectra in the cubic phase indicates that the some interactions occur in the ground state. Furthermore, the emission spectrum largely changes on the cubic–columnar phase transition induced by the mechanical stimulus at room temperature. In the shear-induced columnar phase, the emission peak is observed at 497 nm, which can be ascribed to the interference with the excimer formation of π-conjugated moieties of compound **1**.

To examine the formation of intermolecular hydrogen bond for compound **1**, infrared (IR) spectra of compound **1** were obtained (Fig. 6). The C═O stretching band is observed at 1685 cm^{-1} in the isotropic phase. In the rectangular columnar phase and the cubic phase, the C═O stretching bands are seen at 1651 cm^{-1} and 1650 cm^{-1} respectively. This observation indicates that the intermolecular hydrogen bond is formed in the rectangular columnar phase and in the cubic phase. The C═O and N─H stretching bands in the rectangular columnar phase are sharper than those in the cubic phase, suggesting that the cooling process from

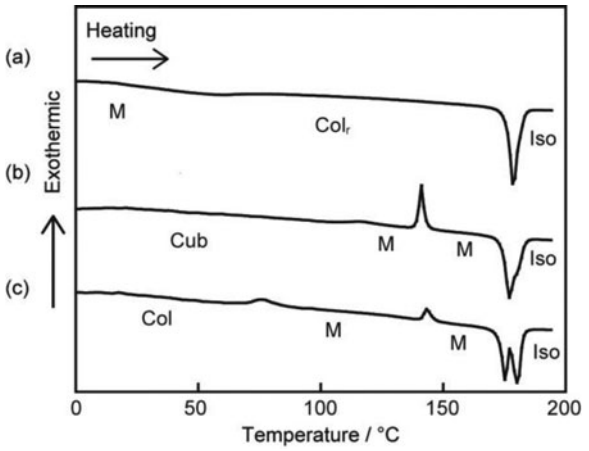

Figure 4. DSC traces on the first heating at the rate of 10°C min^{-1}: (a) sample after slow cooling from the isotropic phase; (b) sample after rapid cooling from the isotropic phase; (c) sheared sample in cubic phase at r.t.

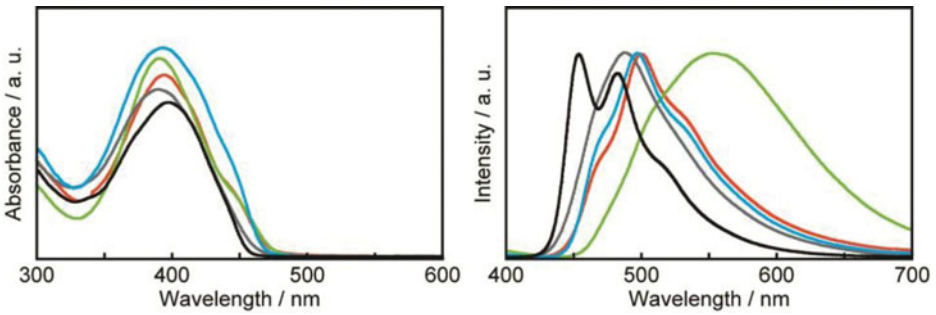

Figure 5. Absorption (a) and emission (b) spectra of compound **1** in the chloroform solution (1.0×10^{-5} M, black), in the isotropic phase at 200°C (gray), in the rectangular columnar phase at 170°C (red), in the cubic phase at r.t. (green), and in the shear-induced columnar phase at r.t. (blue). $\lambda_{ex} =$ 380 nm.

the isotropic phase affects the self-assembled structures in the LC phases at the molecular level. In the shear-induced columnar phase, the peak of the C=O stretching band shifts to 1656 cm^{-1} and an additional shoulder is appeared at 1682 cm^{-1}, suggesting that the hydrogen bond becomes weaker and some free amide groups exist in the shear-induced columnar phase. This behavior is different from the our previous results [3, 23–25]. The stimuli-responsive properties can be tuned by using different π-conjugated molecules as the core of this molecular system consisting of the bulky dendrimer moiety.

The assembled structures of the π-conjugated moieties in the LC phases are proposed in Fig. 7. In the rectangular columnar phase, the amide groups form linear and uniform

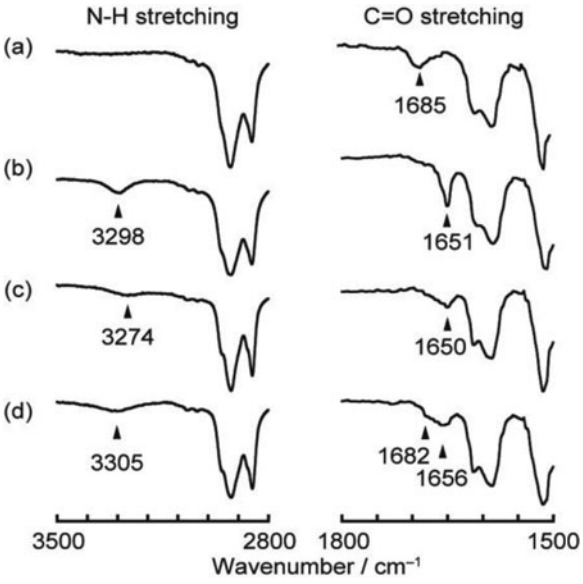

Figure 6. IR spectra of compound **1**: (a) in the isotropic phase at 200°C; (b) in the rectangular columnar phase at 170°C; (c) in the cubic phase at r.t. and (d) in the shear-induced columnar phase at r.t.

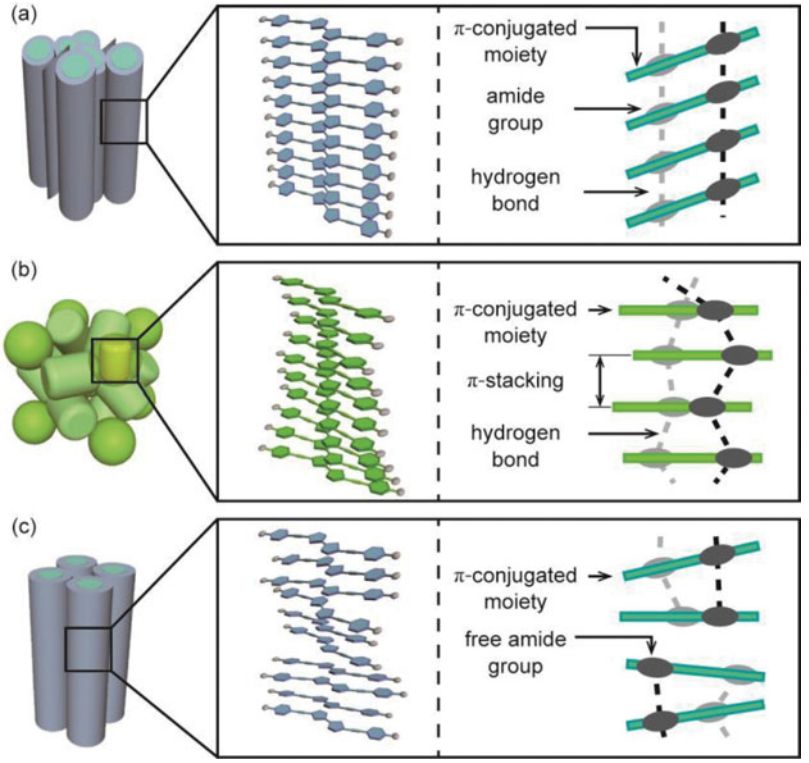

Figure 7. Schematic illustrations of the assembled structures of the π-conjugated moieties of compound **1**: (a) rectangular columnar phase; (b) cubic phase and (c) shear-induced columnar phase. Amide groups of compound **1**: gray spheres. π-Conjugated moieties of compound **1**: blue and green planes. Right: side views of the columns and micelles.

hydrogen bonds between the adjacent molecules, as indicated by IR measurements. The formation of linear hydrogen bonds induces the tiled π-π stacking, resulting in the interference with the excimer formation. This proposed assembled structure (Fig. 7) is supported by previous reports on the crystal structures of arenedicarboxamides [42]. In the cubic phase, π-π stacked structures are formed, leading to the formation of the excimer as indicated by the broad and structureless emission spectrum. Disordering in stacked π-moieties occurs because the lengths of π-π stacking is shorter than those of amide. The broad C=O stretching band in the IR spectrum (Fig. 6) supports the proposed assembled structures. In the shear-induced columnar phase, the formation of the excimer is disturbed due to partial dissociation of hydrogen bond.

Conclusions

Stimuli-responsive liquid crystal **1** based on the bithiophene moiety was obtained. Compound **1** shows the mechanochromic photoluminescent behavior at room temperature on the cubic–columnar phase transition. The mechanism of the photoluminescent color change is based on the change of the assembled structures of the π-conjugated moieties. IR measurements show that the intermolecular hydrogen bond is formed in the cubic phase and mechanical stimulus induces the partial deformation of the intermolecular hydrogen

bond. We are studying on the electronic functions of compound **1** for the application to the sensing devices.

Acknowledgments

This work was partially supported by a Grant-in-Aid for a Scientific Research (no. 22107003) in the Innovative Area of "Fusion Materials" (area no. 2206) and Exploratory Research (no. 22655061) from the Ministry of Education, Culture, Sports, Science and Technology (MEXT). M. M. is grateful for financial support from the Japan Society for the Promotion of Science (JSPS) Research Fellowship for Young Scientists and JSPS Program for Leading Graduate Schools (MERIT).

References

[1] Löwe, C., & Weder, C. (2002). *Adv. Mater.*, *14*, 1625.
[2] Mizukami, S., Houjou, H., Sugaya, K., Tokuhisa, H., Sasaki, T., & Kanesato, M. (2005). *Chem. Mater.*, *17*, 50.
[3] Sagara, Y., & Kato, T. (2008). *Angew. Chem. Int. Ed.*, *47*, 5175.
[4] Sagara, Y., Mutai, T., Yoshikawa, I., & Araki, K. (2007). *J. Am. Chem. Soc.*, *129*, 1520.
[5] Ito, H., Saito, T., Oshima, N., Kitamura, N., Ishizaka, S., Hinatsu, Y., Wakeshima, M., Kato, M., Tsuge, K., & Sawamura, M. (2008). *J. Am. Chem. Soc.*, *130*, 10044.
[6] Kunzelman, J., Kinami, M., Crenshaw, B. R., Protasiewicz, J. D., & Weder, C. (2008). *Adv. Mater.*, *20*, 119.
[7] Sagara, Y., & Kato, T. (2009). *Nat. Chem.*, *1*, 605.
[8] Zhang, G., Lu, J., Sabat, M., & Fraser, C. L. (2010). *J. Am. Chem. Soc.*, *132*, 2160.
[9] Yoon, S.-J., Chung, J. W., Gierschner, J., Kim, K. S., Choi, M.-G., Kim, D., & Park, S. Y. (2010). *J. Am. Chem. Soc.*, *132*, 13675.
[10] Tsukuda, T., Kawase, M., Dairiki, A., Matsumoto, K., & Tsubomura, T. (2010). *Chem. Commun.*, *46*, 1905.
[11] Chi, Z., Zhang, X., Xu, B., Zhou, X., Ma, C., Zhang, Y., Liu, S., & Xu, J. (2012). *Chem. Soc. Rev.*, *41*, 3878.
[12] Demus, D., Goodby, J. W., Gray, G. W., & Spiess, H.-W. (1998). *Handbook of Liquid Crystals*, Wiley-VCH, Weinheim.
[13] Gray, G. W. (1987). *Thermotropic Liquid Crystals*, Wiley, Chichester.
[14] Yang, D.-K., Chien, L.-C., & Doane, J. W. (1992). *Appl. Phys. Lett.*, *60*, 3102.
[15] Mizoshita, N., Hanabusa, K., & Kato, T. (1999). *Adv. Mater.*, *11*, 392.
[16] Takezoe, H., & Takanishi, Y. (2006). *Jpn. J. Appl. Phys.*, *45*, 597.
[17] Kato, T. (2002). *Science*, *295*, 2414.
[18] Kato, T., Mizoshita, N., & Kishimoto, K. (2006). *Angew. Chem. Int. Ed.*, *45*, 38.
[19] Wiesenauer, B. R., & Gin, D. L. (2012). *Polym. J.*, *44*, 461.
[20] Cho, B.-K. (2012). *Polym. J.*, *44*, 475.
[21] Yoshizawa, A. (2012). *Polym. J.*, *44*, 490.
[22] Eimura, H., Yoshio, M., Shoji, Y., Hanabusa, K., & Kato, T. (2012). *Polym. J.*, *44*, 594.
[23] Sagara, T., Yamane, S., Mutai, T., Araki, K., & Kato, T. (2009). *Adv. Funct. Mater.*, *19*, 1869.
[24] Sagara, Y., & Kato, T. (2011). *Angew. Chem. Int. Ed.*, *50*, 9128.
[25] Sagara, Y., & Kato, T. (2011). *Supramol. Chem.*, *23*, 310.
[26] Kozhevnikov, V. N., Donnio, B., & Bruce, D. W. (2008). *Angew. Chem. Int. Ed.*, *47*, 6286.
[27] Yamane, S., Tanabe, K., Sagara, Y., & Kato, T. (2012). *Top. Curr. Chem.*, *318*, 395.
[28] Funahashi, M. (2009). *Polym. J.*, *41*, 459.
[29] Pisula, W., Zorn, M., Chang, J.-Y., Müllen, K., & Zentel, R. (2009). *Macromol. Rapid. Commun.*, *30*, 1179.
[30] O'Neill, M., & Kelly, S. M. (2011). *Adv. Mater.*, *23*, 566.

[31] Yasuda, T., Ooi, H., Morita, J., Akama, Y., Minoura, K., Funahashi, M., Shimomura, T., & Kato, T. (2009). *Adv. Funct. Mater.*, *19*, 411.
[32] Matsui, A., Funahashi, M., & Kato, T. (2010). *Chem. Eur. J.*, *16*, 13465.
[33] Nuita, M., Sakuda, J., Hirai, Y., Funahashi, M., & Kato, T. (2011). *Chem. Lett.*, *40*, 412.
[34] Yasuda, T., Shimizu, T., Liu, F., Ungar, G., & Kato, T. (2011). *J. Am. Chem. Soc.*, *133*, 13437.
[35] Fichou, D. (2000). *J. Mater. Chem.*, *10*, 571.
[36] Hotta, S., & Waragai, K. (1993). *Adv. Mater.*, *5*, 896.
[37] Garnier, F., Yassar, A., Hajlaoui, R., Horowitz, G., Deloffre, F., Servet, B., Ries, S., & Alnot, P. (1993). *J. Am. Chem. Soc.*, *115*, 8716.
[38] Dodabalapur, A., Torsi, L., & Katz, H. E. (1995). *Science*, *268*, 270.
[39] Meng, Q., Gao, J., Li, R., Jiang, L., Wang, C., Zhao, H., Liu, C., Li, H., & Hu, W. (2009). *J. Mater. Chem.*, *19*, 1477.
[40] Kozma, E., Munno, F., Kotowski, D., Bertini, F., Luzzati, S., & Catellani, M. (2010). *Synth. Met.*, *160*, 996.
[41] Percec, V., Cho, W.-D., Ungar, G., & Yeardley, D. J. P. (2001). *J. Am. Chem. Soc.*, *123*, 1302.
[42] Lewis, F. D., Yang, J.-S., & Stern, C. L. (1996). *J. Am. Chem. Soc.*, *118*, 12029.